

- P. Cohen, *Biochem. Biophys. Acta* **1178**, 189 (1993); C. Sutherland, D. G. Campbell, P. Cohen, *Eur. J. Biochem.* **212**, 581 (1993); P. Dent *et al.*, *Nature* **348**, 302 (1990).
8. R. J. Wiese *et al.*, *J. Biol. Chem.* **270**, 3442 (1995); T. Lin and J. C. Lawrence Jr., *ibid.* **269**, 21255 (1994); L. J. Robinson, Z. F. Razzack, J. C. Lawrence, D. E. James, *ibid.* **268**, 26422 (1993).
 9. D. F. Lazar *et al.*, *ibid.* **270**, 20801 (1995).
 10. 3T3-L1 fibroblasts were induced to differentiate into adipocytes as described (9), and polyadenylated [poly(A⁺)] mRNA was obtained with the Messenger RNA Isolation kit (Stratagene, La Jolla, CA). Poly(A⁺) mRNA (5 µg) was used to synthesize cDNA with the Stratagene cDNA synthesis kit. cDNA fragments were then ligated unidirectionally into Eco RI-Xho I-digested pGAD-GH GAL4 activation domain plasmid (Clontech, Palo Alto, CA).
 11. A Gal4p-DNA-binding domain (BD) fusion of PP1C was constructed by cloning the entire PP1α open reading frame, contained within a 1.0-kb Eco RI-Bam HI fragment, into the Eco RI-Bam HI sites of pGBT9 (Clontech), creating BD-PP1C. Strain Y190 was transformed first with BD-PP1C, Trp⁺ prototrophs were selected, and then strain Y190 was transformed with 150 µg of 3T3 L1 adipocyte library DNA. Transformants were selected by plating cells on synthetic medium lacking tryptophan, leucine, and histidine (SD-Trp-Leu-His) and containing 25 mM 3-aminotriazole. Colonies that appeared after 5 days of incubation at 30°C were patched onto SD-Trp-Leu-His plates and then replica-plated onto M63GV-Trp-Leu-His media containing 5-bromo-4-chloro-3-indolylphosphate-β-D-galactopyranoside (X-Gal; Gibco-BRL) for preliminary determination of β-Gal activity. Of ~3.5 × 10⁵ total transformants, 64 His⁺ prototrophic colonies were recovered, of which 27 were β-Gal-positive.
 12. M. Kozak, *J. Cell Biol.* **108**, 229 (1989).
 13. J. M. Francois *et al.*, *EMBO J.* **11**, 87 (1992).
 14. J. A. Printen, M. J. Brady, A. R. Saltiel, data not shown.
 15. B. C. Reed, S. H. Kaufmann, J. C. Mackall, A. K. Student, M. D. Lane, *Proc. Natl. Acad. Sci. U.S.A.* **74**, 4876 (1977); C. S. Rubin, A. Hirsch, C. Fung, O. M. Rosen, *J. Biol. Chem.* **253**, 7570 (1978); A. G. de Herreros and M. J. Birnbaum, *ibid.* **264**, 19994 (1989).
 16. The FLAG-epitope (NH₂-DYKDDDDK-COOH) was introduced into pCI-neo (Promega, Madison, WI) by ligating complementary oligonucleotides into Nhe I-Eco RI-digested vector. A 1.0-kb Eco RI fragment from clone B1-1 was cloned in-frame at the Eco RI site of the resulting plasmid, producing plasmid pF-PTG. The FLAG-PTG fusion is expressed from the strong cytomegalovirus (CMV) enhancer-promoter.
 17. S. B. Waters, K. Yamauchi, J. E. Pessin, *Mol. Cell. Biol.* **15**, 2791 (1995).
 18. CHO-IR cells transfected with pFPTG were sonicated in PP1 homogenization buffer (9) and centrifuged at 14000g for 10 min at 4°C to remove nuclei and cell debris. FLAG-PTG was immunoprecipitated from the supernatant by incubation with 10 µg of anti-FLAG (Kodak, New Haven, CT) for 1 hour at 4°C. Immune complexes were precipitated by incubation with protein A/G-agarose for 1 hour at 4°C and washed four times with homogenization buffer before the addition of SDS-sample buffer. Immunoprecipitates and subcellular fractions were separated on SDS-polyacrylamide gels, transferred to nitrocellulose, and probed with either FLAG monoclonal antibody or with affinity-purified polyclonal antibody to PP1.
 19. CHO-IR cells were washed three times with ice-cold phosphate-buffered saline, scraped in homogenization buffer, and samples sonicated and centrifuged at 2500g to remove nuclei and unlysed cells. The postnuclear supernatant was removed and centrifuged for 15 min at 10,000g and 1 hour at 100,000g to pellet plasma membranes and glycogen pellets, respectively. The final supernatant was called cytosol.
 20. A 1.0-kb Eco RI fragment from clone B1-1, encoding residues 8 to 293 of PTG, was subcloned into the Eco RI site of pGEX-5X-3 expression vector. The GST-PTG fusion protein was expressed in *Escherichia coli* BL21(DE3)LysS and purified by affinity chromatography on glutathione-Sepharose beads.
 21. Glycogen synthase: 100 µl of GST-PTG or GST-PTP1B (20 µg) bound to glutathione-Sepharose beads was resuspended in 725 µl of glycogen synthase buffer [50 mM Hepes (pH 7.8), 100 mM NaF, 10 mM EDTA] plus 25 µl (0.1 U) of purified glycogen synthase (Sigma), followed by incubation at 4°C for 1 hour with gentle mixing. The Sepharose beads were washed four times with glycogen synthase buffer, brought to a final volume of 300 µl, and 50 µl assayed for glycogen synthase activity by measuring the incorporation of uridine 5'-diphosphate (UDP)-[¹⁴C]glucose into glycogen, in the presence and absence of 10 mM glucose-6-phosphate. Phosphorylase: 50 µl of fusion protein beads were added to 750 µl of homogenization buffer containing 0.15 M NaCl, 0.1% bovine serum albumin (BSA), and 25 µg of ³²P-labeled phosphorylase a. The tubes were incubated at 4°C for 1 hour, washed four times with homogenization buffer, and proteins were separated by SDS-PAGE, followed by autoradiography. Phosphorylase kinase: Fusion protein beads (50 µl) were incubated with 10 µg of purified phosphorylase kinase (Gibco-BRL) in homogenization buffer plus 0.15 M NaCl and 0.1% BSA, incubated for 30 min at 4°C, and washed four times with the same buffer. Ten microliters of beads and 2 µg of phosphorylase b were assayed for 5 min at 37°C in 50 mM Hepes (pH 7.4), 10 mM MgCl₂, 1 µM okadaic acid, and 20 µM [γ-³²P]ATP (4000 cpm/pmol), in the absence (1 mM EGTA) or presence (0.5 mM) of Ca²⁺. At the end of the incubation period SDS-sample buffer was added, proteins were separated by SDS-PAGE, and radiolabeled phosphorylase a was visualized by autoradiography and quantitated by scintillation counting.
 22. E. G. Krebs *et al.*, *Biochemistry* **3**, 1022 (1964).
 23. Glycogen synthase, phosphorylase kinase, and PKA assays: 3T3-L1 adipocytes were lysed in 1 ml of homogenization buffer and incubated with 25 µg of fusion protein immobilized on glutathione-Sepharose beads for 1 hour at 4°C. The beads were washed four times with homogenization buffer and assayed for bound glycogen synthase in the presence of glucose-6-phosphate (9). Phosphorylase kinase activity was determined as above (21). PKA activity was determined with bacterially expressed NH₂-terminal portion of RG1 (5 µg) in the presence and absence of 0.1 mM dibutyryl-cyclic AMP (dbcAMP). PP1 and PP2A: 3T3-L1 adipocytes were lysed in 1 ml of homogenization buffer and incubated as above with fusion protein. After extensive washing, the beads were assayed for phosphatase activity in the presence of 0, 3, and 500 nM okadaic acid. Activity loss between 0 and 3 nM is attributed to PP2A activity; loss between 3 and 500 nM is due to PP1 activity (2). Okadaic acid (500 nM) completely inhibited all phosphatase activity on the beads or in the starting extract.
 24. H. Shima *et al.*, *Biochem. Biophys. Res. Commun.* **192**, 1289 (1993); H. Shima *et al.*, *ibid.* **194**, 930 (1993).
 25. S. Shenolikar and A. C. Nairn, *Adv. Second Messenger Phosphoprotein Res.* **23**, 1 (1991); S. Shenolikar, *Annu. Rev. Cell Biol.* **10**, 55 (1994).
 26. A. R. Saltiel, *FASEB J.* **8**, 1034 (1994).
 27. We thank M. Chang for the pCI-neo/FLAG construct, A. Nairn for PP1α cDNA, and J. Lawrence for antibodies to PP1Cα and glycogen synthase.

10 September 1996; accepted 27 January 1997

Block in Anaphase Chromosome Separation Caused by a Telomerase Template Mutation

Karen E. Kirk,* Brian P. Harmon, Isabel K. Reichardt, John W. Sedat, Elizabeth H. Blackburn†

Telomeres are essential for chromosome stability, but their functions at specific cell-cycle stages are unknown. Telomeres are now shown to have a role in chromosome separation during mitosis. In telomeric DNA mutants of *Tetrahymena thermophila*, created by expression of a telomerase RNA with an altered template sequence, division of the germline nucleus was severely delayed or blocked in anaphase. The mutant chromatids failed to separate completely at the midzone, becoming stretched to up to twice their normal length. These results suggest a physical block in mutant telomere separation.

Telomeres "cap" the termini of eukaryotic chromosomes. Chromosomes lacking telomeres undergo fusion, degradation, and extremely high loss rates (1-3). However, there is little information on the mechanism by which telomeres ensure chromosome stability, or at what cell-cycle

stage their job is performed.

In the ciliated protozoan *Tetrahymena thermophila* the transcriptionally active, polygenomic macronucleus divides amitotically, whereas the diploid germline micronucleus, with its chromosomal complement of five pairs of metacentric chromosomes, divides mitotically (4). The telomeric DNA tracts of the two nuclei have the same terminal GGGGTT repeat sequence, although the tracts are markedly different in overall length (5). Whereas macronuclear telomeres play a crucial role in amitotic macronuclear divisions (6), the function of micronuclear telomeres has not been examined. Micronuclear chromosomes are transcriptionally quiescent and mostly dispensable for vegeta-

K. E. Kirk, I. K. Reichardt, E. H. Blackburn, Department of Microbiology and Immunology, University of California, San Francisco, 513 Parnassus, Box 0414, San Francisco, CA 94143-0414, USA.

B. P. Harmon and J. W. Sedat, Department of Biochemistry and Biophysics, University of California, San Francisco, 513 Parnassus, Box 0554, San Francisco, CA 94143-0414, USA.

*Present address: Department of Biology, Lake Forest College, Lake Forest, IL 60045, USA.

†To whom correspondence should be addressed.

tive cell divisions (7), facilitating studies of the role of telomeres in mitotic chromosome stability.

In *T. thermophila*, the wild-type (WT) telomerase RNA (TER1 RNA) contains the template sequence for the synthesis of GGGGTT telomeric repeats. Mutating this sequence generates corresponding mutations in the telomeric DNA (6). In this study, the template was changed to a sequence predicted to synthesize GGGGTTTT telomeric repeats, and this mutated gene, *ter1-43AA*, was introduced on a high-copy vector into WT *T. thermophila* cells (8). Four days after transformation with *ter1-43AA*, many cells were enlarged, and the cell population doubling rate was much slower than that of control cells transformed with WT *TER1* (9). By 5 days, most *ter1-43AA* transformants were grossly enlarged and misshapen (Fig. 1), and their doubling rate had markedly decreased (9). The cells ceased to divide within 18 to 30 population doublings after transformation, except for rare revertants arising from

loss of the introduced *ter* gene (9). This gradual onset of cell death, reminiscent of previously characterized telomerase RNA mutants in *Tetrahymena* (6), is interpreted as a cumulative effect of the cells using the altered telomerase during growth.

Five days after transformation, the fraction of *ter1-43AA* transformant cells with micronuclei in mitotic anaphase (Fig. 1, F and G) was over fivefold higher than in WT transformants, indicating a severe delay or block at this stage of the cell cycle. Furthermore, the anaphase micronuclei in many highly enlarged mutant cells appeared stretched out and were up to twice as long as wild-type anaphase micronuclei (compare Fig. 1G to Fig. 1D), but with no visible separation of chromosomes at the midzone. These results suggested that the mutant telomeres prevented complete chromosome segregation. The proportions of elongated (Fig. 1F) and "hyperelongated" (Fig. 1G) micronuclei, taken as an average from quantitation of seven independent cell lines 7 days after transformation, were 26 and 25%, respectively, resulting in an average total mitotic index of 51% (10). In contrast, quantitation of WT micronuclei demonstrated an average of 7% elongated micronuclei, and none was hyperelongated. These data, coupled with an ~16-hour population doubling time (WT transformant

control doubling time was ~4 hours) (9), indicated that the average time in anaphase for *ter1-43AA* micronuclei was ~8 to 9 hours—nearly 30 times longer than the 15- to 20-min anaphase of WT micronuclei. The hyperelongation of mutant micronuclei indicated that anaphase in the mutant cells continued to progress despite the failure of chromatids to separate.

To study the structure of the *ter1-43AA* anaphase micronuclei, we used three-dimensional, high-resolution wide-field fluorescence microscopy (11). The *ter1-43AA* micronuclei were hyperelongated, and the distances between the leading edges (the centromeres) were ~15 and ~17 μm , respectively (Fig. 2, A and B). However, the daughter chromosome sets were still unseparated. In contrast, WT anaphase micronuclei with a comparable distance (15 μm) between leading centromeres showed a pronounced (2.7 μm) gap between the trailing free chromosome ends (Fig. 2E). Chromosome strands in the *ter1-43AA* hyperelongated micronuclei nearly always appeared continuous, and sometimes tautly stretched from one pole to the other, with no obvious separation between chromatids (Fig. 2A). Rarely, one free chromosome end was clearly detected, in an anaphase figure that otherwise showed an overall lack of chromosome segregation between the daughter

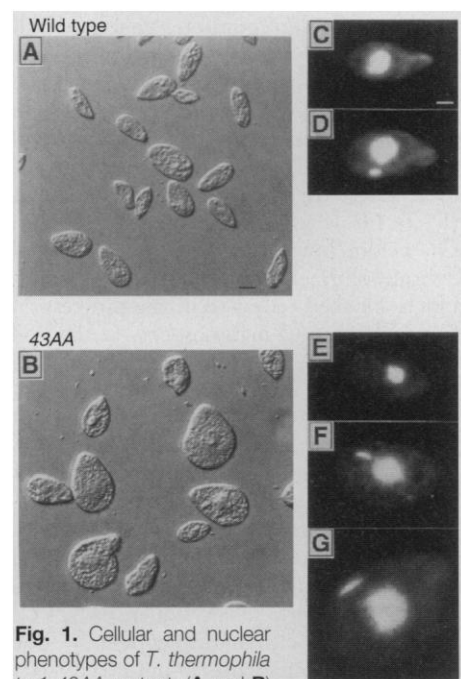
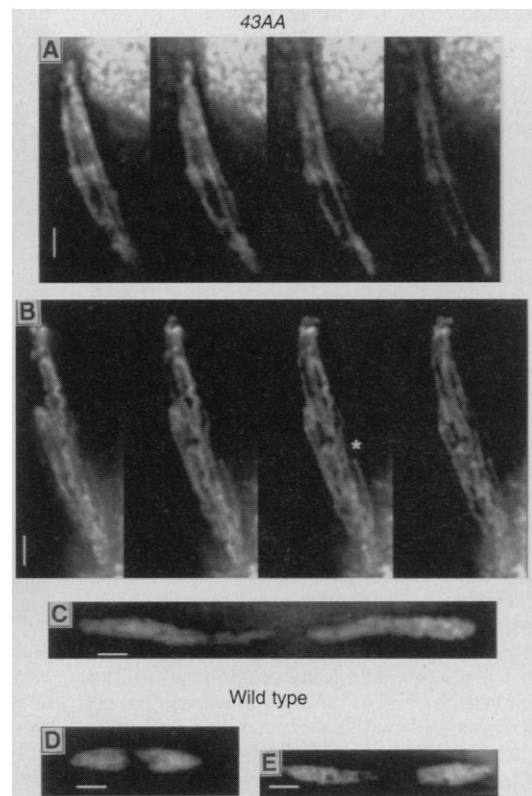


Fig. 1. Cellular and nuclear phenotypes of *T. thermophila ter1-43AA* mutant. (A and B) Nomarski optics (same magnification; bar, 20 μm). (C to G) 4',6'-Diamidino-2-phenylindole (DAPI) fluorescence (same magnification; bar, 10 μm). (A, C, and D) *Tetrahymena thermophila* cells 5 days after transformation with the WT *ter1* gene. (B, E to G) *Tetrahymena thermophila* cells 5 days after transformation with the *ter1-43AA* gene. Cells were fixed in 3.7% formaldehyde in buffer A [15 mM Pipes (pH 7.0), 80 mM KCl, 20 mM NaCl, 0.5 mM EGTA, 2 mM EDTA, 0.5 mM spermidine, 0.2 mM spermine, 1 mM dithiothreitol] and stained with DAPI (0.25 $\mu\text{g}/\text{ml}$). In (C) and (E), interphase micronuclei are positioned in a pocket immediately adjacent to the macronucleus, at roughly 7 and 11 o'clock, respectively. In (D), (F), and (G), elongated micronuclei are indicative of anaphase.

Fig. 2. High-resolution fluorescence microscopy of micronuclei in anaphase. (A to C) *ter1-43AA* micronuclei. (D to E) Wild-type micronuclei in control cells. Cells were fixed, stained with a 1:1000 dilution of Oli-Green (Molecular Probes, Eugene, Oregon), and washed in buffer A. Cells were pipetted onto polylysine (1 mg/ml)-coated #1.5 cover slips, allowed to dry briefly, and layered with 20 μl of fluorescence mounting medium (Vectashield; Vector Laboratories, Burlingame, California). Subsequent control studies indicated that the drying step did not significantly affect the data qualitatively or quantitatively (27). Three-dimensional (3D) data sets were collected with an Olympus 60 \times 1.4 numerical aperture oil immersion lens on a computer-controlled wide-field microscopy system and cooled charge-coupled device (CCD) camera (11). Cells were imaged in 3D by moving the sample through the focal plane of the objective lens at 0.25- μm increments and recording an image with the CCD camera at each position. Out-of-focus light was removed by a constrained iterative deconvolution algorithm with an empirical point-spread function (28). Processed data were examined and manipulated by means of the IVE software package developed for 3D images (29). (A) and (B) are serial projections, where 12 sequential single-plane images 0.25 μm thick are converted into four sequential projections 0.75 μm thick. In (B), a free end is marked (*). (C) to (E) are single-plane images. Bars, 2 μm .



poles (Fig. 2B, asterisk). This observation, and inspection of large numbers of mutant cell anaphase figures, indicated that separation of sister chromatids was detectable by this imaging method and was rare. Several thousand mutant anaphase micronuclei were scanned, but only one showed chromosome separation at the midzone (Fig. 2C). This midzone gap measured 2.8 μm , yet the distance between the leading daughter centromeres was 27 μm —nearly twice the distance between the centromeres in WT nuclei with comparably separated daughter chromatids. In WT anaphase micronuclei, the chromatid arms were generally not individually resolved. In contrast, in the hyperelongated mutant micronuclei, individual strands, possibly representing multiple arms bundled together, were readily visualized. Their number varied between anaphase micronuclei, perhaps reflecting chromosome missegregation in the *ter1-43AA* mutant.

To investigate whether the block in micronuclear mitosis in the *ter1-43AA* mutant caused the gradual cell death observed, we quantitated the micronuclear phenotype and cell division capability of transformant lines. Random single cells were isolated and scored for these properties 24 hours after isolation. In all seven transformant cell lines analyzed in one experiment, although different lines varied quantitatively, the frequency of hyperelongated micronuclei correlated strongly with cell death. For example, on day 5, most C7 transformant line cells were grossly enlarged, with 50% of the visible micronuclei in mitotic anaphase, and 50% of these being hyperelongated

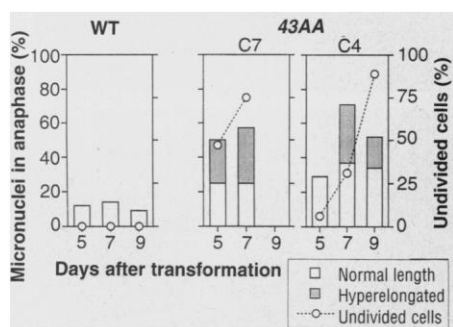


Fig. 3. Micronuclear hyperelongation correlates with lack of cell division. After the establishment of transformed cell lines, the cell concentration was monitored and cells were diluted as needed into fresh medium containing paromomycin (100 $\mu\text{g}/\text{ml}$). At 5, 7, and 9 days after electroporation, (i) the phenotype of 60 micronuclei on average per cell line was assessed for elongation and hyperelongation as described (10), and (ii) individual cells were isolated to determine division capability. For the latter analysis, 35 random single cells per cell line were isolated into fresh medium and division was scored 24 hours later.

(Fig. 3). Of the single cells isolated at this time point, 47% remained undivided 24 hours later. On day 7, 75% failed to divide, and all cells had ceased dividing by day 9. In contrast, on day 5, the C4 cellular phenotype was less severe, and only 6% failed to divide, but on day 7, large numbers of hyperelongated micronuclei had appeared, and fewer cells divided. On day 9, many C4 cell nuclei appeared degraded, and nearly all cells failed to divide (Fig. 3). Together, these data strongly suggest that the extreme lag or block in micronuclear anaphase of *ter1-43AA* mutants caused the block in cell division.

The nuclear and cellular phenotypes of *ter1-43AA* mutant cells allowed inference of their cellular progression (Fig. 4). In WT *Tetrahymena* cells, the micronucleus completes mitosis before the macronucleus undergoes its amitotic division (12), after which cytokinesis occurs (Fig. 4, A to F). Despite the inability of *ter1-43AA* mutant cells to complete micronuclear division, some aspects of cell cycle progression took place, as evidenced by the extreme stretch-

ing of the mutant anaphase micronucleus, indicating continuation of anaphase (Fig. 4I), visible cleavage furrow initiation (Fig. 4, H and I), and grossly enlarged cytoplasm (Fig. 4J). Such cell cycle progression is predicted, because in ciliates, commitment to cell division occurs during micronuclear anaphase (13). The *ter1-43AA* cells that had reached a terminal phenotype (unable to divide, but still motile) were usually grossly enlarged and misshapen, with both nuclei visibly degraded (Fig. 4K). In many such cells, the micronucleus was no longer visible and the macronucleus was splayed and partially fragmented. An alternative terminal phenotype was an unusually small, misshapen cell containing an interphase micronucleus or no visible micronucleus (9). Both terminal phenotypes accounted for the lack of further increase in mitotic micronuclei 7 to 9 days after transformation (Fig. 3).

These findings provide strong evidence that a mutant telomeric DNA sequence, generated by the expression of an altered telomerase RNA, causes a severe delay or block in completing mitotic anaphase. Although the sister chromatids begin to separate and are pulled apart as anaphase progresses, they are unable to segregate to the daughter poles. What is the nature of the anaphase arrest? A DNA damage cell-cycle arrest triggered by mutant telomeres (2, 3, 14) would be expected to occur in G_2 , before mitosis (15). In contrast, cell division of the *Tetrahymena ter1-43AA* mutant is blocked only late in the progression of anaphase, and many aspects of the cell cycle continue. These results, and the extremely high failure rate of chromatid separation, are consistent with a physical block in telomere separation during or before anaphase. Therefore, we propose that telomeres of sister chromatids normally are associated until metaphase, and that resolution of this association before chromosome segregation in anaphase is abrogated by the mutated telomeric DNA sequence.

How sister chromatids cohere to one another until anaphase is unknown (16–18), but telomeres may be involved. Normal telomere-telomere associations, seen cytologically in a variety of organisms (19) and occurring specifically in G_2 in *Schizosaccharomyces pombe* (20), could be mediated through single-stranded DNA tails (21) or telomere-binding factors. The latter include the TBP proteins of hypotrichous ciliates, the Rap1p or Sir proteins of yeasts, and hTRF of humans (22, 23), or the telomerase ribonucleoprotein itself. A failure of telomere separation in the *ter1-43AA* mutant could result from covalent fusion of the mutant telomeric DNA, or it could be mediated through aberrant association of telo-

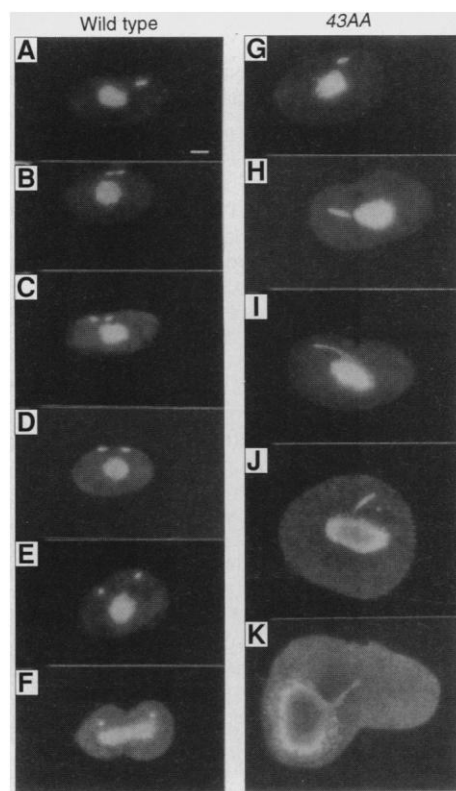


Fig. 4. Fluorescence microscopy indicates *ter1-43AA* micronuclei remain blocked in anaphase as cell cycle progresses. *Tetrahymena thermophila* cells transformed with (A to F) the WT *ter1* gene and (G to K) the *ter1-43AA* gene (same magnification, bar, 10 μm). Cells were stained with DAPI as described in the legend to Fig. 1 and images of different cells were compiled into an inferred progression.

mere-binding factors. Altered spatial organization in the nucleus, or an altered telomere structure, could also make mutant telomeres inaccessible to factors that normally act to separate sister chromatids. For example, the yeast DNA untangler topoisomerase II is required for anaphase chromatid separation (24), as is proteolysis of noncyclin proteins such as Cut2 (18, 25). The *cut2* and *cut1* mutant phenotype (26) is strikingly similar to that of *Tetrahymena ter-43AA*: The main bodies of the sister chromosomes are pulled apart, but the telomeres remain localized late in anaphase, while the cell cycle continues (20). Further investigations into cells with altered telomere structure will help define the mechanism by which sister chromatids cohere and separate in a timely manner.

REFERENCES AND NOTES

1. E. H. Blackburn and C. W. Greider, Eds., *Telomeres* (Cold Spring Harbor Laboratory Press, Cold Spring Harbor, NY, 1995).
2. L. L. Sandell and V. A. Zakian, *Cell* **75**, 729 (1993).
3. M. J. McEachern and E. H. Blackburn, *Genes Dev.* **10**, 1822 (1996).
4. J. G. Gall, Ed., *Molecular Biology of Ciliated Protozoa* (Academic Press, New York, 1986).
5. K. E. Kirk and E. H. Blackburn, *Genes Dev.* **9**, 59 (1995).
6. G.-L. Yu, J. D. Bradley, L. D. Attardi, E. H. Blackburn, *Nature* **344**, 126 (1990).
7. P. J. Bruns, T. B. Brussard, E. V. Merriam, *Genetics* **104**, 257 (1983).
8. The template sequence of the *T. thermophila* WT telomerase RNA gene (*ter1*) was mutated from 5'-(43)-CAACCCCAA-3' to 5'-(43)AAAACCCCAA-3', by means of polymerase chain reaction, and the mutated gene (*ter1-43AA*) was cloned into the vector pRD4-1 [D. Gilley and E. H. Blackburn, *Mol. Cell. Biol.* **16**, 66 (1996)]. *Tetrahymena thermophila* strains CU428 and B2086 were mated and transformed by electroporation [J. Gaertig and M. A. Gorovsky, *Proc. Natl. Acad. Sci. U.S.A.* **89**, 9196 (1992)], with pter1-43AA. Control cells were transformed by electroporation with the WT telomerase RNA gene [pTer1; G.-L. Yu, J. D. Bradley, L. D. Attardi, E. H. Blackburn, *Nature* **344**, 126 (1990)]. Selection was initiated 16 hours after electroporation by the addition of paromomycin (100 µg/ml; Sigma). Four days after electroporation, 20 individual *ter1-43AA* transformant cell lines were pooled, and growth was continued for two additional days. Total DNA was isolated [D. P. Romero and E. H. Blackburn, *J. Eukaryot. Microbiol.* **42**, 32 (1995)]. Telomeric DNA was cloned into pBluescript (Stratagene), and the library then screened with a G₄T₄-specific oligonucleotide. Because the transformed cells also retain their endogenous chromosomal copy of the WT telomerase RNA gene, both WT and mutant repeats are synthesized onto the telomeres. A total of 115 telomeric repeats were sequenced from three different macronuclear telomere clones, 23% of which were mutated. The mutated repeats were confined almost exclusively to the most distal region of the telomere.
9. K. E. Kirk and E. H. Blackburn, unpublished data.
10. Micronuclear phenotypic quantitation was performed in over 700 cells from 14 independent transformant cell lines in two separate experiments from 5 to 7 days after transformation. On average, 55 random micronuclei per cell line per time point were assessed for anaphase by 4',6'-diamidino-2-phenylindole (DAPI) stain. Cells with no visible micronuclei were excluded from the determination. Length was judged by eye to be roughly equivalent to that observed in WT (elongated) or at least 50% longer

- than that found in WT, with no apparent separation at the midzone (hyperelongated). The proportion of micronuclei in anaphase varied with respect to cell line and time point (standard deviations for elongated and hyperelongated micronuclei at 7 days were ±7% and ±16%, respectively).
11. Y. Hiraoka, J. R. Swedlow, M. R. Paddy, D. A. Agard, J. W. Sedat, *Semin. Cell Biol.* **2**, 153 (1991).
12. In the *ter1-43AA* mutant, the macronucleus was never observed to divide while the micronucleus was arrested in anaphase. Hence, the onset of macronuclear division may require completion of micronuclear division. Therefore, although mutant telomeres also impair macronuclear division (6), possibly independently of the micronuclear telomere phenotype, such impairment of macronuclear division may not become evident while the micronucleus is mitotically blocked.
13. S. M. Adl and J. D. Berger, *J. Eukaryot. Microbiol.* **43**, 77 (1996).
14. T. A. Weinert, G. L. Kiser, L. H. Hartwell, *Genes Dev.* **8**, 652 (1994).
15. T. A. Weinert, *Radiat. Res.* **132**, 141 (1992).
16. C. Holm, *Cell* **77**, 955 (1994).
17. W. Y. Miyazaki and T. L. Orr-Weaver, *Annu. Rev. Genet.* **28**, 167 (1994).
18. M. Yanagida, *Bioessays* **17**, 519 (1995).
19. A. F. Dernberg, J. W. Sedat, W. Z. Cande, H. W. Bass, in (1), pp. 295–338.
20. H. Funabiki, I. Hagan, S. Uzawa, M. Yanagida, *J. Cell Biol.* **121**, 961 (1993).

21. E. Henderson, in (1), pp. 11–34.
22. G. Fang and T. R. Cech, in (1), pp. 69–106.
23. L. Chong et al., *Science* **270**, 1663 (1995).
24. W. C. Earnshaw and A. M. Mackay, *FASEB J.* **8**, 947 (1994).
25. H. Funabiki et al., *Nature* **381**, 438 (1996).
26. T. Hirano, S.-I. Funahashi, T. Uemura, M. Yanagida, *EMBO J.* **5**, 2973 (1986).
27. Cells were also imaged under wet buffer conditions without drying and were found to be quantitatively and qualitatively identical to dried cells: Anaphase micronuclei lengths were on average 10.46 µm by 2.06 µm by 2.49 µm for nondried (*n* = 7) and 10.95 µm by 1.98 µm by 2.23 µm (*n* = 3) for dried; nondried chromosomes were 0.41 ± 0.09 µm wide (*n* = 69) versus 0.40 ± 0.07 µm wide for dried chromosomes (*n* = 35).
28. D.A. Agard, Y. Hiraoka, P. Shaw, J. W. Sedat, *Methods Cell Biol.* **30**, 353 (1989); Y. Hiraoka, J. W. Sedat, D. A. Agard, *Biophys. J.* **57**, 325 (1990).
29. H. Chen, D. D. Hughes, T.-A. Chan, J. W. Sedat, D. A. Agard, *J. Struct. Biol.* **116**, 56 (1996).
30. We thank J. C. Prescott, A. Bhattacharyya, and H. W. Bass for manuscript review. Supported by NIH grant GM26259 (to E.H.B.), an American Cancer Society postdoctoral fellowship (to K.E.K.), and by an NSF predoctoral fellowship (to B.P.H.).

7 November 1996; accepted 23 January 1997

Immune Hyperactivation of HIV-1-Infected T Cells Mediated by Tat and the CD28 Pathway

Melanie Ott, Stephane Emiliani, Carine Van Lint, Georges Herbein, Jennie Lovett, Narendra Chirmule, Thomas McCloskey, Savita Pahwa, Eric Verdin*

Human immunodeficiency virus–type 1 (HIV-1) infection is characterized by a chronic state of immune hyperactivation in patients. Infection of human peripheral blood lymphocytes with HIV-1 in vitro resulted in increased interleukin-2 (IL-2) secretion in response to T cell activation via the CD3 and CD28 receptors. Expression of the HIV-1 transactivator Tat recapitulated this phenotype and was associated with increased IL-2 secretion in response to costimulation with CD3 plus CD28. IL-2 superinduction by Tat occurred at the transcriptional level, was mediated by the CD28-responsive element in the IL-2 promoter, and was exclusively dependent on the 29 amino acids encoded by the second exon of Tat.

Symptoms of immune hyperactivation in HIV-1-infected individuals are noted throughout the course of infection and include spontaneous lymphocyte proliferation; expression of T cell activation antigens; lymph node hyperplasia; increased cytokine expression; and elevated levels of neopterin, β₂-microglobulin, acid-labile interferon, and IL-2 receptors (1, 2). Immune hyperactivation is probably critical for the maintenance of the infectious process, as

HIV-1 cannot infect resting T cells (3, 4) and therefore depends on a pool of activated T cells in the host. Proposed mechanisms for this immune hyperactivation include the persistence of virus and viral antigens throughout the course of the disease, the presence of a superantigen encoded by HIV or another microbe, and the presence of autoimmune phenomena (2).

We considered the possibility that HIV-1 infection itself could lead to the superactivation of infected T cells. Peripheral blood lymphocytes (PBLs) were infected with the primary viral isolate HIV-1_{89.6} (5) after activation with antibodies to CD3. Cells were then restimulated with antibodies directed against the CD3 and CD28 molecules. These two receptors play a critical role in T cell activation; the CD3

M. Ott, S. Emiliani, C. Van Lint, G. Herbein, J. Lovett, E. Verdin, The Picower Institute for Medical Research, 350 Community Drive, Manhasset, NY 11030, USA. N. Chirmule, T. McCloskey, S. Pahwa, North Shore University Hospital and New York University School of Medicine, 350 Community Drive, Manhasset, NY 11030, USA.

*To whom correspondence should be addressed. E-mail: verdin@picower.edu